Thermolysis of Polyhedral Oligomeric Silsesquioxane (POSS) Macromers and POSS−Siloxane Copolymers

R. A. Mantz,† P. F. Jones, K. P. Chaffee, J. D. Lichtenhan,* and J. W. Gilman‡

Phillips Laboratory, Propulsion Directorate, Edwards AFB, California 93524

I. M. K. Ismail and M. J. Burmeister

Hughes STX, Phillips Laboratory, Propulsion Directorate, Edwards AFB, California 93524

Received November 13, 1995. Revised Manuscript Received March 15, 1996⊗

The pyrolysis of four polyhedral oligomeric silsesquioxane (POSS) macromers, $Cy_8Si_8O_{11}(OH)_2$, $Cy_8Si_8O_{11}(OSiMe_3)_2$, $Cy_6Si_6O_9$, and $Cy_8Si_8O_{12}$ (where Cy = *c*-C_6H_{11}) and two POSS−siloxane copolymers [$Cy_8Si_8O_{11}$−$(OSiMe_2)_nO$−] (n = 1, oligomer average 5.4) has been studied in argon, nitrogen, and under vacuum from 30 to 1000 °C. Product gases were analyzed by TGA-FTIR and mass spectroscopy. Analysis of the chars was conducted using cross-polarized (CP) and magic angle spinning (MAS) NMR spectroscopy, X-ray diffraction, density measurements, and gas adsorption analysis. All of the POSS macromers showed a propensity toward sublimation, while the POSS-siloxane copolymers underwent a complex depolymerization−decomposition process. For the copolymer [$Cy_8Si_8O_{11}$−$(OSiMe_2)_{5.4}O$−] this process included the evolution of cyclic dimethylsiloxanes at 400 °C, cyclohexyl hydrocarbons from 450 to 550 °C, and H_2 liberation from 700 to 1000 °C. Loss of the silsesquioxane "cage" structure occurred upon heating from 450−650 °C and after the evolution of most of the pyrolysis gases. Changes in both char porosity and density accompanied the structural rearrangements. The activation energies for pyrolysis under argon or nitrogen was 56 ± 9 kcal/mol and for oxidation in air was 20 ± 4 kcal/mol.

Introduction

Investigation of the thermal decomposition processes for polymeric systems can provide insight into the structure, composition, thermal stability, and thermochemistry of new macromolecular materials.[1] The development of graftable and polymerizable polyhedral oligomeric silsesquioxane (POSS) macromers based on structurally well-defined silsesquioxane precursors are examples of new polymer building blocks which promise the preparation of a wide variety of novel polymeric compositions.[2] Previous studies into the thermolysis of polyhedral silsesquioxanes[3] and polysilsesquioxanes[4] have primarily focused on the preceramic nature of silsesquioxanes toward the formation of SiO_xC_y chars and SiC ceramics. While providing great insight into the polymer−ceramic conversion process, the previous studies[4] have been confounded by a detailed knowledge of only these materials compositions, with little knowledge regarding the materials actual polymeric structures. It is the intent of this study to provide an examination of the thermochemical properties for structurally and compositionally well-defined silsesquioxane materials based on POSS building blocks. In this work our objective has been 2-fold: (1) to compare the thermochemistry of POSS macromers to POSS-siloxane copolymers and (2) to determine the fate of the POSS cage structure throughout the process leading to char formation.

Experimental Section

Materials. The POSS macromers $Cy_8Si_8O_{11}(OH)_2$,[5] $Cy_8Si_8O_{11}(OSiMe_3)_2$,[6] $Cy_6Si_6O_9$,[5,7] and POSS−siloxane copolymers [$Cy_8Si_8O_{11}$−$(OSiMe_2)_nO$−] (n = 1, oligomer average 5.4)[8] were prepared according to literature methods. The compound $Cy_8Si_8O_{12}$ was prepared in a manner slightly different from that reported previously.[7] $Cy_7T_7(OH)_3$ (5.14 mmol, 5.00 g) and triethylamine (15.4 mmol, 1.56 g) were dissolved in 40 mL of THF and stirred in an ice bath. A solution of *c*-$C_6H_{11}SiCl_3$ (5.28 mmol, 1.14 g) dissolved in 20 mL of THF was added dropwise to the mixture over 5 min. Immediate precipitation of white solids was observed. The mixture was allowed to warm to room temperature and react for 10 h. The precipitate was removed through filtration and the filtrate was taken to dryness under vacuum (recovered 5.56 g crude). To remove traces of $(CH_3CH_2)_3NHCl$ and $(CH_3CH_2)_3N$, the crude material was dissolved in chloroform (150 mL) and extracted repeatedly

† Currently at North Carolina State University, Raleigh, NC 27695.
‡ Currrently at NIST, Gaithersburg, MD 20899-0001.
* To whom correspondence should be addressed.
⊗ Abstract published in *Advance ACS Abstracts,* May 1, 1996.

(1) Mittlemann, M. L.; Johnson, D.; Wilkie, C. A. *Trends Polym. Sci.* **1994**, *2*, 391.
(2) Lichtenhan, J. D. *Comments Inorg. Chem.* **1995**, *17*,115.
(3) Feher, F. J.; Weller, K. J. *Chem. Mater.* **1994**, *6*, 7. Banaszak Holl, M. M.; Read McFreely, F. *Phys. Rev. Lett.* **1993**, *71*, 2441. Lee, S.; Makan, S.; Banaszak Holl, M. M.; Reed McFeely, F. *J. Am. Chem. Soc.* **1994**, *116*, 11819.
(4) Burns, G. T.; Taylor, R. B.; Xu, Y.; Zangvil, A.; Zank, G. A. *Chem. Mater.* **1992**, *4*, 1313. Laine, R. M.; Rahn, J. A.; Youngdahl, K. A.; Babonneau, F.; Hoppe, M. L.; Zhang, Z.-F.; Harrod, J. F. *Chem. Mater.* **1990**, *2*, 464. Rahn, J. A.; Laine, R. M.; Zhang, Z.-F. *Mater. Res. Soc. Symp. Proc.* **1990**, *171*, 31. Hurwitz, F. I.; Heimann, P.; Farmer, S. C.; Hembree, Jr., D. M. *J. Mater. Sci.* **1993**, *28*, 6622.
(5) Feher, F. J.; Newman, D. A.; Walzer, J. F. *J. Am. Chem. Soc.* **1989**, *111*, 1741.
(6) Feher, F. J.; Newman, D. A. *J. Am. Chem. Soc.* **1990**, *112*, 1931.
(7) Brown, Jr., J. F.; Vogt, Jr., L. H. *J. Am. Chem. Soc.* **1965**, *87*, 4313.
(8) Lichtenhan, J. D.; Vu, N. Q.; Carter, J. A.; Gilman, J. W.; Feher, F. J. *Macromolecules* **1993**, *26*, 2141.

S0897-4756(95)00536-9 CCC: $12.00

with water (3 × 100 mL). The organic layer was isolated and dried over $MgSO_4$ for 12 h. This solution was then decanted, the solvent removed under vacuum, and the residue redissolved in THF, filtered, and dried under vacuum to give 5.40 g of white powder (97%). ^{1}H NMR ($CDCl_3$) $\delta = 1.65$ (m, 40 H; H_{eq}), $\delta = 1.17$ (m, 40 H; H_{ax}), $\delta = 0.67$ (m, 8 H; H_{ipso}). ^{13}C NMR $\delta = 27.51, 26.91, 26.66, 23.21$. ^{29}Si NMR (relative to $SiMe_4$ in $CDCl_3$) $\delta = -68.63$. The X-ray powder diffraction pattern for this product also matched that previously reported.[9]

Thermogravimetric Analysis (TGA). Thermolysis reactions were studied using two different TGA apparatus. The first was a Cahn-2000 TGA connected to a high-vacuum system. To remove trapped gases from the samples, they were evacuated (1 h at 10^{-4} Torr) and then flushed with ultrahigh-purity argon or nitrogen. Depending on the type of run (pyrolysis or oxidation) the samples were heated under a gas flowing at 50 cm^3/min and then heated at a fixed rate (0.25−20 °C/min), from room temperature to 1000 °C. To eliminate buoyancy effects, the final weights of the chars were obtained after cooling the char back to room temperature.

The second TGA apparatus, manufactured by TA Instruments (Model TGA-951), was coupled to an FTIR gas analyzer manufactured by Nicolet, Inc. (Model 7-SX). Samples (5−10 mg) were first flushed with nitrogen at 100 cm^3/min for 30 min and then heated at 10 °C/min from room temperature to 1000 °C under nitrogen. Evolved gases from the sample were swept through a heated (250 °C) capillary transfer line to a gas analysis cell and then to the spectrometer sample compartment by nitrogen purge gas. FTIR spectra were recorded once every 6 s at an instrument resolution of 8 cm^{-1}.

Surface Area and Porosity Determinations. Samples for surface area and porosity measurements were prepared in a horizontal quartz reactor ($1^3/_8$ in. i.d., 4 ft length) heated in a tubular furnace. A 3.0 g polymer sample was charged into the reactor, flushed with argon (25 °C, 50 cm^3/min) for 1 h and then partially pyrolyzed isothermally (stepwise) for 1 h at each of several temperatures: 450, 475, 500, 525, 550, 575, 600, 625, 650, and 675 °C. After terminating the partial pyrolysis at each designated temperature, the sample was cooled in argon to room temperature, a small fraction was saved for density determination, and the remaining sample was taken for surface area and porosity measurements. Surface area and porosity determinations were made using N_2 and CO_2 as the adsorbates. Upon completion of these measurements, the sample was placed back into the quartz reactor and heated isothermally to the next (higher) pyrolysis temperature.

The adsorption measurements on the partially pyrolyzed polymer samples were obtained using a Micromeritics Digisorb 2600 surface area analyzer. Before each measurement, the sample was evacuated for 3 h at 100 °C. The adsorption isotherms of nitrogen at −196 °C were obtained in order to estimate the surface area and pore volumes of each sample, taking into account that the density of liquid nitrogen filling the pores was 0.808 g/cm^3, and the cross-sectional area of an adsorbed molecule in the monolayer was 0.162 nm^2.[10] The BET (Brunauer−Emmett−Teller) equation[11] was used to compute the total surface area, which encompasses the external area of the particles plus the internal areas inside micropores, (<2.0 nm width), mesopores (2.0−50.0 nm), and macropores (>50.0 nm).[12]

In estimating the micropore volumes and surface areas with CO_2, the values for density and cross-sectional area of an adsorbed molecule were taken as 0.71 g/cm^3 and 0.17 nm^2, respectively. With this adsorbate the Dubinin−Radushkivich equation[13] was used to estimate the limiting micropore volumes and the corresponding surface areas.

Density Measurements. Char densities were determined through suspension of char samples (2−3 mg) in a density gradient column composed of benzene ($d = 0.879$ g/mL) and bromoform ($d = 2.890$).[14] Char samples were allowed to equilibrate in the mixture for 24 h.

Stepwise Isothermal Pyrolysis. Polymer pyrolysis was also carried out in a static reactor operating at subambient pressures. In a quartz boat, 10−15 mg of the polymer was evacuated (12 h, 10^{-7} Torr) then heated stepwise at 50, 100, or 200 °C increments from room temperature to 1000 °C. At each isothermal temperature, the sample was held for 35 min in order to perform a two-step gas analysis. First, with the cold trap at −196 °C, the noncondensable gases were analyzed and then pumped out of the system. Gases were also analyzed by removing the −196 °C bath, allowing the trap to warm to ambient temperature, and then sampled and pumped out of the system. The procedure for gas analysis involved removal of a cold trap, expansion of condensed vapors, analysis, and reevacuation of the system before the sample was heated to the next higher temperature. At each temperature, the pressure was noted and the evolved products were analyzed with a residual gas analyzer mass spectrometer (UTI Model 100C). The micromoles of gas liberated at each temperature was computed from the measured system pressure and the calibrated volumes of the system components (reactor, manifold, and cold trap).

Preparation of Chars for NMR Experiments. Bulk char samples were prepared in a nitrogen purged furnace which was heated at 15 °C/min to the desired temperature. Samples were held for 0.1 h and then cooled under nitrogen purge to room temperature. A small portion of each resulting char was subsequently analyzed by the TGA to verify the temperature the sample had reached in the purge furnace. A portion of the remaining sample was ground and used for solid-state NMR and X-ray diffraction experiments.

NMR. Solid-state CPMAS ^{29}Si NMR spectra were recorded on a Bruker AMX FT-NMR spectrometer at 59.62 MHz. To obtain quantitative peak areas and to maximize the signal to noise ratio a study was performed on $[Cy_8Si_8O_{11}-(OSiMe_2)_{5.4}O-]$ in which the cross polarization contact time was varied.[15] The optimum cross polarization contact time was determined to be 2 ms. Where appropriate, cross polarization/magic angle spinning was employed.[16] Under these conditions 256 scans were acquired with a relaxation delay of 10 s. When necessary only magic angle spinning was used. Under these conditions 1000 scans were acquired with a relaxation delay of 60 s. All chemical shifts were externally referenced to $Si_8O_{20}(SiMe_3)_8$.

Solution ^{1}H, ^{13}C, ^{29}Si NMR spectra were obtained on the same instrument at 300.13 and 75.47 MHz, respectively. ^{1}H and ^{13}C chemical shifts are reported relative to the residual protons in the respective NMR solvent. For ^{29}Si NMR spectra, chemical shifts are reported relative to tetramethylsilane dissolved in $CDCl_3$ and used as an external reference.

X-ray Powder Diffraction. Measurements were performed using a Scintag D5000 $\theta-\theta$ diffractometer system using Ni filtered Cu Kα radiation (1.5406 Å). Samples were ground to 200 mesh (74 μm) and were then spread thinly on a zero-background plate. Data were recorded with a Braun scanning PSD system operating with a 10% methane in argon balance counting gas. Integration times were 200 s/pt.

Results and Discussion

Monomer/Polymer Pyrolysis and Analysis of Gas-Phase Products. Thermolysis studies on the

(9) Barry, A. J.; Daudt, W. H.; Dominicone, J. J.; Gilkey, J. W. *J. Am. Chem. Soc.* **1965**, *77*, 3990.

(10) Gregg, S. J.; Sing, K. S. *Adsorption, Surface Area and Porosity*, 2nd ed.; Academic Press: New York, 1982.

(11) Brunauer−Emmett−Teller (BET) equation: Brunauer, S.; Emmett, P. H.; Teller, E. J. *J. Am. Chem. Soc.* **1938**, *60*, 309.

(12) Sing, K. S.; Everett, D. H.; Haul, R. A.; Moscou, L.; Pierotti, R. A.; Rouquerol, J.; Siemieniewska, T. *J. Pure Appl. Chem.* **1985**, *57*, 603.

(13) Dubinin−Radushkivich (DR) equation: Dubinin, M. M.; Zaverina, E. D.; Radushkevich, L. V. *Zh. Fiz. Khim.* **1947**, *21*, 1351.

(14) Method D 1505-68, Annual Book of ASTM Standards, 1985; Section 8.01, p 683.

(15) Voelkel, R. *Angew. Chem., Int. Ed. Engl.* **1988**, *27*, 1468. Alemany, L. B.; Grant, D. M.; Pugmire, R. J.; Alger, T. D.; Zilm, K. W. *J. Am. Chem. Soc.* **1983**, *105*, 2133.

(16) Schaefer, J.; Stejskal, E. O.; Buchdahl, R. *Macrololecules* **1995**, *8*, 291.

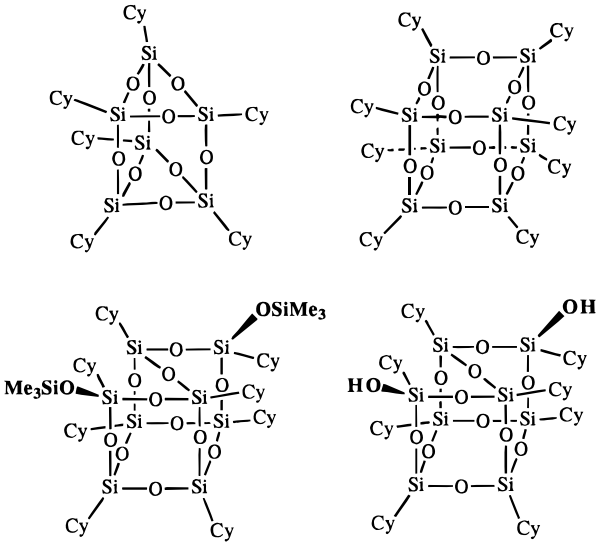

Figure 1. POSS macromers studied include $Cy_6Si_6O_9$, $Cy_8Si_8O_{12}$ and $Cy_8Si_8O_{11}(OSiMe_3)_2$, $Cy_8Si_8O_{11}(OH)_2$.

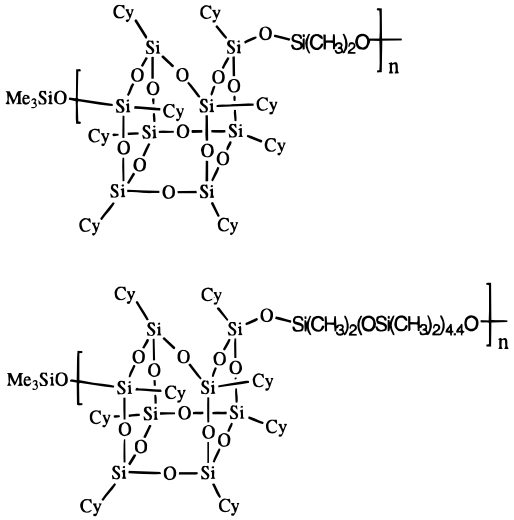

Figure 2. POSS−siloxane copolymers studied include $[Cy_8Si_8O_{11}-(OSiMe_2)_1O-]$ and $[Cy_8Si_8O_{11}-(OSiMe_2)_{5.4}O-]$.

series of POSS macromers (Figure 1) and on the POSS−siloxane copolymers (Figure 2) were conducted. It was believed that analysis of the decomposition processes for the macromers would provide insight into decomposition pathways of the linear POSS−siloxane copolymers. This type of information could aid in the design of future POSS polymers with enhanced thermal stability.

The four POSS macromers shown in Figure 1 are all colorless crystalline solids which appear white in a powdered form. This series allows for a comparison of the thermal properties of POSS macromers relative to their silicon−oxygen cage structure and substituent functionality. The $Cy_6Si_6O_9$ and $Cy_8Si_8O_{12}$ (Cy = *c*-C_6H_{11}) systems represent fully condensed structures absent of reactive substituents. In contrast, the $Cy_8Si_8O_{11}(OH)_2$ and $Cy_8Si_8O_{11}(OSiMe_3)_2$ systems have incompletely condensed structures and contain functionalities useful in polymerizations. Such functionalities may also play a role in subsequent thermal decomposition pathways.

The POSS−siloxane copolymers shown in Figure 2 are also colorless solids; however, in contrast to the macromers, they are amorphous in nature. The physical characteristics of the two polymer systems differ in that $[Cy_8Si_8O_{11}-(OSiMe_2)_1O-]$ is a brittle solid while $[Cy_8Si_8O_{11}-(OSiMe_2)_{5.4}O-]$ is a modestly flexible thermoplastic.

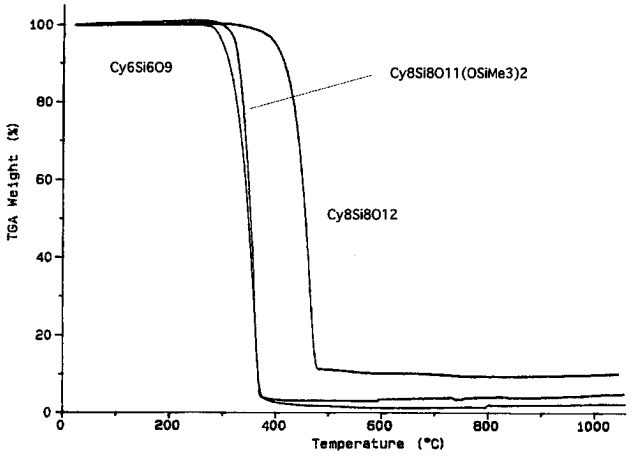

Figure 3. TGA overlay for $Cy_6Si_6O_9$, $Cy_8Si_8O_{12}$, and $Cy_8Si_8O_{11}(OSiMe_3)_2$.

TGA plots for three of the macromers are shown in Figure 3. The compounds $Cy_6Si_6O_9$, $Cy_8Si_8O_{12}$, and $Cy_8Si_8O_{11}(OSiMe_3)_2$ were observed to sublime at ambient pressure under nitrogen at 359, 463, and 360 °C, respectively. Progression of the temperature maximum for sublimation is consistent with the increased molecular weight of $Cy_8Si_8O_{12}$ (1081 amu) over $Cy_6Si_6O_9$ (811 amu). The observation of a lower maximum sublimation temperature for $Cy_8Si_8O_{11}(OSiMe_3)_2$ (1244 amu) contrasts to its mass relationship with $Cy_6Si_6O_9$ and $Cy_8Si_8O_{12}$. However, the reduced molecular symmetry and the presence of two bulky trimethylsilyl groups likely prevents $Cy_8Si_8O_{11}(OSiMe_3)_2$ from packing as efficiently. The gas-phase FTIR spectra for each of these compounds was observed to match the FTIR spectrum obtained for pelletized authentic samples and supports our conclusion that the samples do not undergo thermal decomposition at these temperatures.[17] Sublimation of the fully condensed POSS systems was expected given previously reported observations.[18] However, sublimation of incompletely condensed POSS (i.e., $Cy_8Si_8O_{11}(OSiMe_3)_2$) structures at ambient pressure without inducing structural rearrangements has now been observed.

A TGA plot and first derivative curve for the macromer $Cy_8Si_8O_{11}(OH)_2$ are shown in Figure 4. The presence of two distinctive mass-loss regions at 230−450 and 450−650 °C suggests a more complicated process than was observed for the silylated analogue $Cy_8Si_8O_{11}(OSiMe_3)_2$.

To probe the processes corresponding to the first mass loss region, samples of $Cy_8Si_8O_{11}(OH)_2$ were heated under a nitrogen atmosphere to 390 °C in a quartz tube furnace. After each run a white material had condensed on the walls of the reactor and was rinsed into a vial using tetrahydrofuran and analyzed by ^1H, ^{13}C, and ^{29}Si NMR spectroscopy. The solution ^1H, ^{13}C, and ^{29}Si NMR

(17) As a note in added support, the ^1H, ^{29}Si NMR of the sublimate also matches that for authentic sample.

(18) Korchkov, V. P.; Martynova, T. N. *Russ. J. Appl. Chem.* **1985**, *58*, 1923 translated from *Zh. Prikl. Khim.* **1985**, *58*, 2089. Ton'shin, A. M.; Kamaritskii, B. A; Spektor, V. N. *Russ. Chem. Rev.* **1983**, *52*, 775 (translated from *Uspekhi Khim.* **1983**, *52*, 1365). Voronkov, M. G.; Lavrent'yev, V. I. *Top. Curr. Chem.* **1982**, *102*, 199.

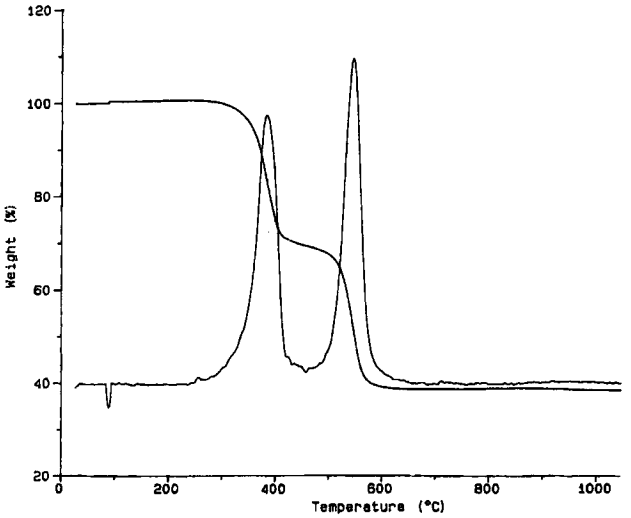

Figure 4. TGA and first-derivative plot for $Cy_8Si_8O_{11}(OH)_2$.

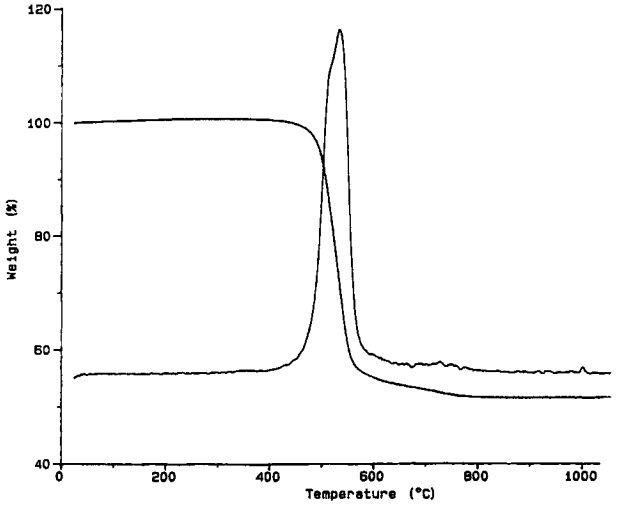

Figure 5. TGA and first-derivative plot for $[Cy_8Si_8O_{11}-(OSiMe_2)_{5.4}O-]$.

spectra for this material was identical with that of authentic $Cy_8Si_8O_{11}(OH)_2$. It was therefore determined that the initial mass-loss region observed in the TGA trace for this compound resulted from sublimation of the $Cy_8Si_8O_{11}(OH)_2$ macromer. Additional confirmation was provided by comparison of the TGA/FTIR spectra of gases evolved in this region to the FTIR spectra obtained for samples of $Cy_8Si_8O_{11}(OH)_2$ pelletized in KBr.

Interestingly, appreciable sublimation of $Cy_8Si_8O_{11}(OH)_2$ was consistently observed only during initial heating of the material from 390 to 450 °C. Heating the compound at temperatures which sustain sublimation but below 390 °C resulted in modest initial sublimation with the process ceasing after several minutes. One explanation for this behavior may be a lowering of initial surface area of the powdered samples through melting and agglomeration. Alternatively, $Cy_8Si_8O_{11}(OH)_2$ may undergo some partial degradation at the sublimation temperatures. Trace amounts of water and carbon dioxide were observed in TGA/FTIR experiments at temperatures up to 450 °C. These products may in fact have resulted from sample degradation. Sublimed $Cy_8Si_8O_{11}(OH)_2$ collected from the reactor walls (mentioned above) showed identical behavior on attempted resublimation. Attempts to reinstate sublimation through grinding of partially sublimed samples had only a limited effect. We conclude that both sublimation and degradation can occur for $Cy_8Si_8O_{11}(OH)_2$ at temperatures below 390 °C.

Attempts to characterize the condensation product of $Cy_8Si_8O_{11}(OH)_2$ have been only modestly successful. The loss of water from $Cy_8Si_8O_{11}(OH)_2$ could result in the formation of the homopolymer $[-O-Cy_8Si_8O_{11}O]_n$. Analysis of the sublimation residue by GPC reveals an increased average molecular weight and a broad distribution. However, all attempts to synthesize the homopolymer $[-O-Cy_8Si_8O_{11}O]_n$ from $Cy_8Si_8O_{11}(OH)_2$ using solution condensation chemistry have failed.

Analysis of the second mass loss region, from 450 to 600 °C, in Figure 4 by FTIR revealed the primary gaseous products to be cyclohexane and cylcohexene. While a detailed mechanistic investigation into the evolution of the hydrocarbon products was not conducted, a two-step radical mechanism similar to that determined for the pyrolysis of silsesquiazanes ($RSiN_{1.5}$)[19] could explain the formation of both cyclohexene and cyclohexane during thermolysis of these silsesquioxanes. Thus, the hydrocarbons produced during pyrolysis could result from initial homolytic cleavage of the cyclohexyl carbon−silicon bond followed either by proton abstraction to produce cyclohexane or alternatively through β-elimination of a hydrogen atom to form cyclohexene.

Thermolysis of the two POSS−siloxane copolymers was carried out under conditions identical with that utilized for the POSS macromers. The primary difference in composition between the two polymers is the relative mass of the dimethylsiloxane segment (5% and 26%, respectively) located between each of the POSS groups. In the case of $[Cy_8Si_8O_{11}-(OSiMe_2)_1O-]$, each POSS is separated by one dimethylsiloxane unit while an average of 5−6 are present in $[Cy_8Si_8O_{11}-(OSiMe_2)_{5.4}O-]$. Both polymers were end-capped with trimethylsilyl groups to reduce the effect of reactive silanol end groups on the thermolysis.[20,21]

The TGA plot and first derivative curve for $[Cy_8Si_8O_{11}-(OSiMe_2)_{5.4}O-]$ are shown in Figure 5. A notable difference between the TGA trace for the copolymers and the macromers is the absence of a weight loss associated with sublimation. Initial weight loss for $[Cy_8Si_8O_{11}-(OSiMe_2)_{5.4}O-]$ occurs at 390 °C and is fully subsided by 650 °C. Analysis of the gaseous byproducts with TGA-FTIR have attributed the initial mass loss to depolymerization of the oligomeric poly(dimethylsiloxane) comonomer segment to form the cyclic dimethylsiloxane species $(Me_2SiO)_3$ (D_3) and $(Me_2SiO)_4$ (D_4). The temperature range over which D_3 and D_4 are detected in the FTIR is 390−518 °C. The lower vapor pressure of D_3 and D_4 allowed these species to be swept into the gas phase, and their presence was confirmed by FTIR relative to authentic samples.[22]

(19) Burns, G. T.; Angelotti, T. R.; Hanneman, L. F.; Chandra, G.; Moore, J. A. *J. Mater. Sci.* **1987**, *22*, 2609.

(20) End groups significantly effect the stability of PDMS. For example see: Zeldin, M.; Qian, B.-R.; Choi, S. J. *J. Polym. Sci., Polym. Chem. Ed.* **1983**, *21*, 1361.

(21) Differences in molecular weight and polydispersity between the two polymer samples was not expected to significantly influence thermochemistry given previous observations in poly(phenylsilsesquioxane) systems. See: Xisheng, Z.; Lianghe, S.; Shuqing, L.; Yizhen, L. *Poly. Degradation Stability* **1988**, *20*, 157.

Table 1. Summary of Predominant Gas-Phase Products and Corresponding Temperatures

POSS compound	range (°C)[a]	T_{max} (°C)[a]	primary volatiles
$Cy_6Si_6O_9$	230−450	359	sublimed
$Cy_8Si_8O_{12}$	280−490	463	sublimed
$Cy_8Si_8O_{11}(OSiMe_3)_2$	250−415	360	sublimed
$Cy_8Si_8O_{11}(OH)_2$	230−450	383	sublimed/condensation
	450−650	446	*c*-C_6H_{10}, *c*-C_6H_{12}
$[Cy_8Si_8O_{11}-(OSiMe_2)_1O-]$	325−610	532	*c*-C_6H_{10}, *c*-C_6H_{12}
$[Cy_8Si_8O_{11}-(OSiMe_2)_{5.4}O-]$	390−525	518	$(Me_2SiO)_3$,[b] $(Me_2SiO)_4$[b]
	525−650	532	*c*-C_6H_{10}, *c*-C_6H_{12}
	650−800		CH_4
	650−1000		H_2

[a] The maximum temperatures listed here are defined by the maximum of the derivative curve from TGA plots. All measurements were taken at ambient pressure in 100 mL/min flowing nitrogen. [b] Additional confirmation by RGA-MS.

Depolymerization of PDMS has been reported to occur near 340 °C.[20,23] The apparent increased stability of the PDMS segment in $[Cy_8Si_8O_{11}-(OSiMe_2)_{5.4}O-]$ may result from a steric influence by the POSS cage on the depolymerization/cyclization of the poly(dimethylsiloxane) segment, or from the relatively small number of dimethylsiloxane units (5.4) in the PDMS copolymer segment. Increased stability of PDMS to depolymerization has similarly been observed in other systems containing bulky or rigid copolymer segments.[24]

Analysis of the products over the range of 525−650 °C reveals that the primary decomposition products are cyclohexyl derivatives; primarily cyclohexane, cyclohexene, and methylcyclohexane. Continued heating from 650−1000 °C produced small amounts of methane and hydrogen.

Note, in contrast to the apparent high decomposition temperatures observed in the ramped TGA experiments (above), isothermal heating experiments on $[Cy_8Si_8O_{11}-(OSiMe_2)_{5.4}O-]$ have shown that absolute thermal stability, via absolute mass retention, is possible only below 300 °C.

Thermolysis of the copolymer $[Cy_8Si_8O_{11}-(OSiMe_2)_1O-]$ was observed to be nearly identical with that for $[Cy_8Si_8O_{11}-(OSiMe_2)_{5.4}O-]$ with the notable exception that cyclic siloxanes were not evolved throughout the pyrolysis range. Interestingly, sublimation of POSS segments from either of the copolymer samples was not observed. This result is in contrast to pyrolysis studies on methylsilicone resins which have been reported to decompose through elimination of $(CH_3SiO_{1.5})_n$ cages.[25] The evolution of $(CH_3SiO_{1.5})_n$ cages in the previous work could be generated by the action of trace amounts of catalyst (presumably present as active end groups) or the resins may in fact contain such noncovalently bound cage structures.

Table 1 provides a summary of the primary thermolysis products for the POSS macromers and POSS−siloxane copolymers. Our results suggest that once incorporated into a polymeric form, POSS macromers decompose primarily through partial loss of their organic substituents which is then followed by subsequent cross-linking reactions that incorporate the remaining composition into a SiO_xC_y network or char. Similar decomposition processes involving partial loss of organic substituents followed by formation of SiO_xC_y networks have been observed for related polysilsesquioxane resins.[4] Such a pathway would in fact seem to be preferred when the relative bond strengths of silicon−oxygen (128 kcal/mol)[26] and silicon−carbon (88 kcal/mol)[26] are considered and provided that some degree of cross-linking can occur.

Analysis of Chars by NMR and X-ray Diffraction. Further consideration of the thermolysis pathways described above raises the question as to the fate of the POSS silicon−oxygen skeleton during the decomposition process. To this end we subjected char samples of the monomer $Cy_8Si_8O_{11}(OH)_2$ and copolymer $[Cy_8Si_8O_{11}-(OSiMe_2)_{5.4}O-]$ to solid-state NMR and X-ray powder diffraction analysis at various intermediate stages of pyrolysis.

The $Cy_8Si_8O_{11}(OH)_2$ macromer was monitored at 30, 360, 390, 450, 536, and 1000 °C, and selected spectra are shown in Figure 6. ^{29}Si NMR spectra for the monomer up to the 390 °C sample are identical in terms of the features and chemical shift values observed for the silanol T ($\delta = -58.6$) and cyclohexyl-substituted silicon T resonances ($\delta = -65.3, -68.2$). Note that the ^{29}Si NMR spectrum can be divided into four regions where M ($O_{1/2}SiR_3$), 8 to −12 ppm; D ($O_{2/2}SiR_2$) −18 to −55 ppm; T ($O_{3/2}Si-R$), −65 to −85 ppm; Q ($O_{4/2}Si$), −85 to −112 ppm.[27] The onset of resonance broadening begins to appear at 390 °C. At 450 °C, the T-type silanol silicons are observed by ^{29}Si NMR to decrease significantly in intensity while the T-type structure persists. Loss of the silanol resonances likely occurs via condensation reactions with retention of the overall POSS macromer T-type structure. This is supported by the absence of significant broadening of the T-type silicon resonances ($\delta = -68.2$) in the ^{29}Si NMR spectrum of the 450 °C char.

The reduction in intensity for the silanol resonances in the ^{29}Si NMR spectra at 450 °C is also consistent with the observation of trace amounts of water in the TGA/

(22) The evolution of D_3 and D_4 siloxanes was detected in this range for the polymer sample by FTIR and evidenced by the presence of bands at 1020−1010 and 1090−1075 cm^{-1}. D_3 and D_4 siloxanes were also detected by mass spectroscopic analysis of the evolved gas during thermolysis experiments in the static reactor apparatus and evidenced by the mass peaks at 222 and 296 amu.

(23) Kendrick, T. C.; Parbhoo, B.; White, J. W. In *The Chemistry of Organic Silicon Compounds*; Patai, S. Rappoport, Z., Eds.; John Wiley and Sons: New York, 1989; Part 2, pp 1319−1340. David, C. In: *Comprehensive Chemical Kinetics*; Bamford, C. H., Tipper, C. F. H., Eds.; Elsevier Scientific Publishing Co.: Amsterdam, 1975; Vol. 14, p 105.

(24) For increased thermal stability of PDMS in carborane−siloxane systems see: Peters, E. N.; Kawakomi, J. H.; Kwiatkowski, G. T.; Hedaya, E.; Joesten, B. L.; McNeil, D. W.; Owens, D. A. *J. Polym. Sci., Polym. Chem. Ed.* **1977**, *15*, 723.

(25) Schneider, O. *Thermochim. Acta* **1988**, *134*, 269. Blazso', M.; Ga'l, E.; Makarova, N. N. *Polyhedron* **1983**, *2*, 455.

(26) Walsh, R. *Acc. Chem. Res.* **1981**, *14*, 246.

(27) Marsmann, H.; Kintzinger, J. P. *Oxygen-17 and Silicon-29 NMR*; Springer-Verlag: New York, 1981; pp 74−239.

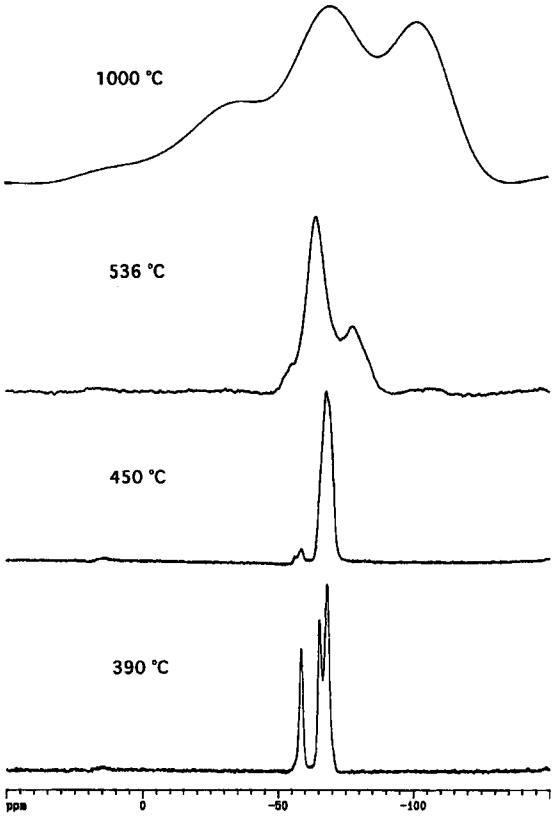

Figure 6. Selected solid-state ^{29}Si NMR of $Cy_8Si_8O_{11}(OH)_2$ chars at successive temperatures.

FTIR experiments over the 390−450 °C range (Figure 4). Elimination of water from $Cy_8Si_8O_{11}(OH)_2$ via a self-condensation polymerization could result in the formation of a $[-O-Cy_8Si_8O_{11}O]_n$ hompolymer. This result would also be consistent with retention of the T-type silicon resonances in the 450 °C ^{29}Si NMR spectrum. Attempts to analyze the 450 °C residue by GPC was thwarted by material insolubility. The reddish-brown color of the sample at this temperature indicates that decomposition in addition to condensation has likely occurred.

Similarly, X-ray diffraction spectra for these char samples show only minimal losses in intensity and broadening of features from 30 °C up to 360 °C (Figure 7). Analysis of the char samples heated to 450 °C via X-ray diffraction reveals that significant crystallinity is still present in the sample. This observation lends further support to retention of the structure present in the original POSS molecule. Interestingly, while crystalline structure persists to the 450 °C level, its lattice dimensions have also slightly changed from those in the original and 360 °C sample.

Continued heating of the chars from 536 to 1000 °C resulted in the partial loss of T-type structure perhaps via the new resonance at $\delta = -77.8$, and the appearance of Q and D-type silicon environments in the ^{29}Si NMR spectrum. Redistribution of the silicon environments is accompanied by dramatic increases in the line widths of features as well as shifts in their maxima values. These changes in the solid-state are not accompanied by significant losses in sample mass in that hydrogen evolution is the primary gas phase product beyond 600 °C. Between 600 and 1000 °C cross polarization of the sample was no longer possible, and by 1000 °C the

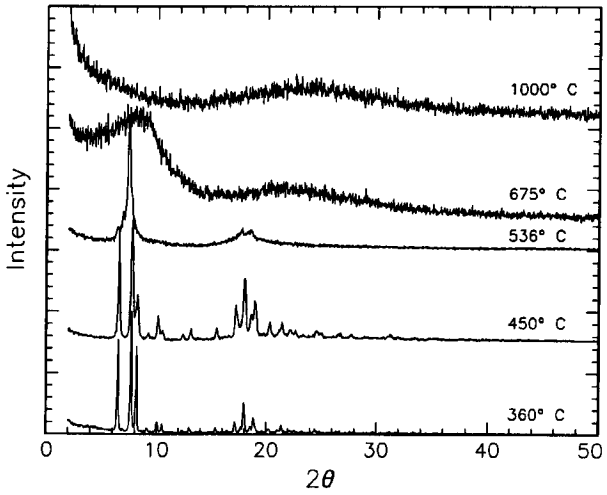

Figure 7. Selected X-ray powder diffraction of $Cy_8Si_8O_{11}(OH)_2$ chars at successive temperatures.

sample contained M, D, T, and Q type silicon environments which is evidence for loss of original structure and scrambling.

The X-ray diffraction spectra for the char samples heated from 536 to 1000 °C clearly show broadened features and a continued conversion of the material from a crystalline to amorphous state. Furthermore, it will be shown in a following section, that the shifting of the diffraction maxima near 18° 2θ to higher values is suggestive of increased densification of the char over this temperature range.

In addition, we have also found that controlled heating of $Cy_8Si_8O_{11}(OH)_2$ in air produces an amorphous material but at much lower temperatures (450 °C) than is observed by heating under an inert atmosphere.

Similarly, investigation of the char material produced from the pyrolysis of the POSS−siloxane copolymer $[Cy_8Si_8O_{11}-(OSiMe_2)_{5.4}O-]$ was conducted using ^{29}Si NMR and X-ray powder diffraction. A sequence of solid-state ^{29}Si NMR spectra for $[Cy_8Si_8O_{11}-(OSiMe_2)_{5.4}O-]$ at intermediate stages of pyrolysis is shown in Figure 8. ^{29}Si NMR spectra for the polymer were observed to be identical from 30 up to 400 °C. The series in Figure 8 reveals the apparent stability of the POSS T-type silicon and the siloxane D-type silicon environments up to >450 °C. As was observed for the POSS monomer, continued heating from 590 to 1000 °C produced polymer decomposition that resulted in a redistribution of the silicon environments along with significant broadening of the ^{29}Si resonances. Analysis of this series of chars by X-ray diffraction (Figure 9) was only modestly informative because of the amorphous nature of the starting polymer. The diffraction spectrum at 430 °C shows two maxima at 8.2 and 17.8° 2θ. Maxima at these scattering angles are typical for POSS-based polymers and are consistent with the presence of POSS cages in the material. Both the X-ray diffraction data and the ^{29}Si NMR spectra of the polymer chars compliment each other with regard to retention and the onset of scrambling/loss of the POSS cage structure. Rearrangement/exchange reactions of the silicon environ-

(28) Belot, V.; Corriu, R. J. P.; Leclercq, D.; Mutin, P. H.; Vioux, A. *J. Mater. Sci. Lett.* **1990**, *9*, 1052. Belot, V.; Corriu, R.; Leclercq, D.; Mutin, P. H.; Vioux, A. *Chem. Mater.* **1991**, *3*, 127. Birot, M.; Pillot, J.-P.; Dunogués, J. *J. Chem. Rev.* **1995**, *95*, 1443.

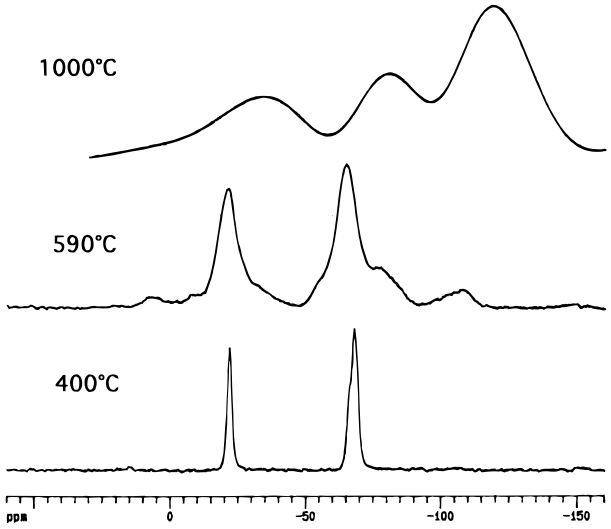

Figure 8. Selected solid-state ^{29}Si NMR of [$Cy_8Si_8O_{11}$−$(OSiMe_2)_{5.4}O$−] chars at successive temperatures.

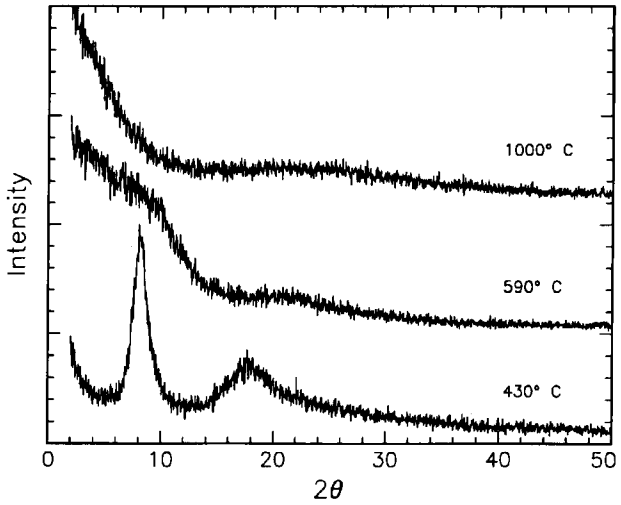

Figure 9. Selected X-ray powder diffraction spectra of [$Cy_8Si_8O_{11}$−$(OSiMe_2)_{5.4}O$−] chars at successive temperatures.

ment at elevated temperatures is common and has been previously observed for silicones, silsesquioxanes, and silane systems.[3,4,28] Additionally, as was observed for the monomer, heating of the polymer char from 600 to 1000 °C increased the density of the material. This density increase was similarly correlated with a shifting of the 18° 2θ diffraction maxima to higher 2θ values.

Consistent with the NMR and X-ray diffraction data, analysis of the resulting 1000 °C char composition by XPS revealed three major silicon environments corresponding to a composition of 14.5% SiO_2, 7.5% SiO_xC_y, and 1.4% SiC. These data are qualitatively consistent with the composition observed by ^{29}Si NMR (Figure 8). Analysis by XPS of the material produced from oxidation of the polymer to 1000 °C resulted in a composition corresponding to 27.0% SiO_2; 0.6% SiO_xC_y, and 0.3% SiC.

Analysis of the ^{29}Si NMR and X-ray spectra over the pyrolysis range 30−1000 °C for both $Cy_8Si_8O_{11}(OH)_2$ and

(29) As an additional note, heating of either the monomer or polymer samples in air did not result in the formation of β-crystobalite. It is well-known, however, that heating amorphous silica for long periods (days−weeks) will promote formation of this form of silica. For example see: Leadbetty, A.; et al. *Nature* **1973**, *244*, 125.

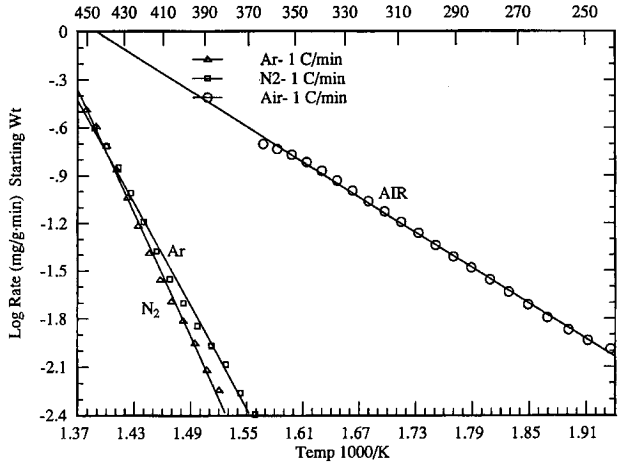

Figure 10. Arrhenius plots for pyrolysis and oxidation of [$Cy_8Si_8O_{11}$−$(OSiMe_2)_{5.4}O$−].

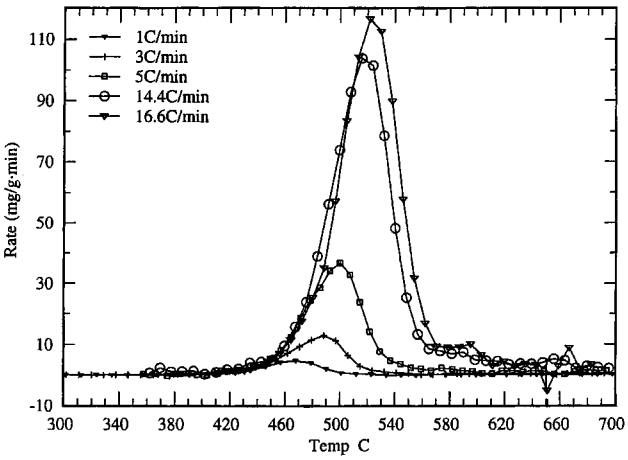

Figure 11. Plots of successive heating rates for [$Cy_8Si_8O_{11}$−$(OSiMe_2)_{5.4}O$−] under nitrogen.

[$Cy_8Si_8O_{11}$−$(OSiMe_2)_{5.4}O$−] reveals several similarities with regard to the fate of the POSS cage structure. Redistribution of the POSS silicon environment for both the monomer and copolymer occurs at approximately 550 °C. Pyrolysis of both monomer and polymer to 1000 °C results in amorphous chars that contain silicon in a wide range of coordinated chemical environments. The relative amounts of D- and T-type silicon present in the initial material composition (POSS monomer or copolymer) does not appear to strongly affect the onset temperature of the redistribution/scrambling reactions. Additionally the D, T ratios present in the initial POSS compositions did not appear to overwhelmingly influence the amount of D, T, and Q structure ultimately produced at 1000 °C.

Pyrolysis and Oxidation Activation Energies. In an attempt to draw comparisons between the thermal stabilities of POSS systems to other polysilsesquioxanes, the activation energies for pyrolysis and oxidation were determined for the copolymer [$Cy_8Si_8O_{11}$−$(OSiMe_2)_{5.4}O$−]. Experiments to determine the activation energies were conducted in a flow reactor under argon and nitrogen, and for oxidation, in air. The activation energy values were calculated in two ways: directly by constructing Arrhenius plots from individual TGA runs (Figure 10) and indirectly using T_{max} for a series of heating rates (Figure 11).

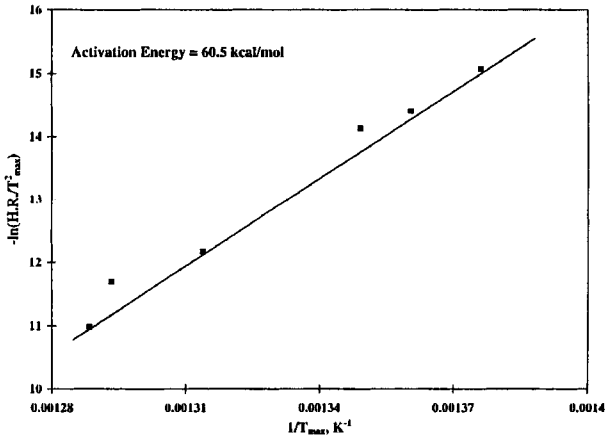

Figure 12. Plot showing first-order pyrolysis of [$Cy_8Si_8O_{11}$−$(OSiMe_2)_{5.4}O$−] in argon.

Reaction rates were computed based on the successive decreasing instantaneous weights of the sample.[30] The activation energies obtained using the direct method (Figure 10) appeared independent of the heating rate, and fluctuated around an average value of 56 ± 9.0 kcal/mol in argon or nitrogen and 20 ± 4 kcal/mol in air. Determinations in air also showed small secondary oxidation reactions above 500 °C. The average activation energy for these reactions was 8kcal/mol. While the value of 20 kcal/mol may be assigned to the oxidation of hydrocarbon groups, the secondary reactions are attributed to partial oxidation of SiO, discrete carbon, and hydrogen.

Plots of heating rate vs temperature in Figure 11 were used in a second method for estimating activation energies. As expected, an increased heating rate shifted the temperatures corresponding to the maximum rate of decomposition, T_{max}, to higher values. After pyrolyzing the polymer at several heating rates, the corresponding values of T_{max} were determined, and the following equation was then applied to estimate the activation energies:[31]

$$A^{-E_a/RT_{max}} = E_a(\text{heating rate}/RT_{max}^2) \qquad (1)$$

where A is the preexponential factor, R is the gas constant, and E_a is the activation energy. If the activation energy is constant at all heating rates and if the decomposition (or oxidation) reaction is assumed to be first order, then the plot of ln(heating rate/RT_{max}^2) versus $1/T_{max}$ is linear.[31] Figures 12 and 13 illustrate these plots for argon and air, respectively.

From the slope of the lines, the activation energies were 61 kcal/mol in argon and 16 kcal/mol in air. The results of both methods are compared in Table 2. In the case of argon, there is an excellent agreement between the 61 kcal/mol value obtained with the T_{max} method and the average value of 56 kcal/mol computed using the direct method, thus confirming that the decomposition of the polymer in inert atmospheres is a first-order reaction.

The activation energy for oxidation in air was determined to be 16 kcal/mol using the indirect method and

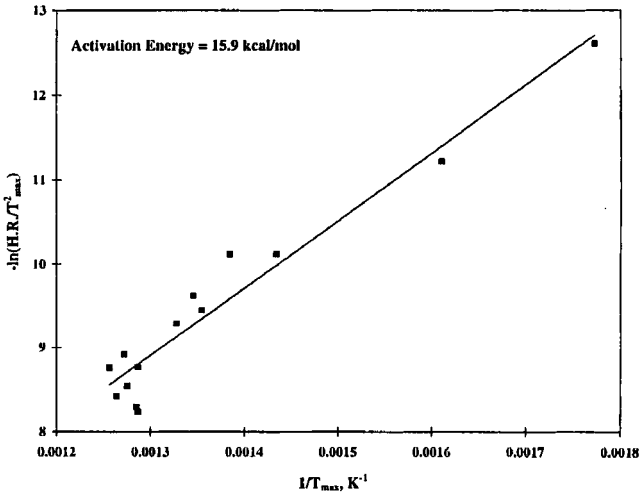

Figure 13. Plot showing first-order oxidation of [$Cy_8Si_8O_{11}$−$(OSiMe_2)_{5.4}O$−] in air.

Table 2. Average Activation Energy (kcal/mol) for Polymer Pyrolysis and Oxidation

method	E_a in Ar or N_2	E_a in air (primary oxidation)
direct	56 ± 9	20 ± 4
indirect (T_{max})	61 ± 5	16 ± 2

20 kcal/mol with the direct method. The discrepancy may in part be explained by realizing that the increased percentage of error in estimating E_a is greater when the value of E_a is small. Additionally, considering that the oxidation reaction involves oxidation of both carbon and silicon, the observed activation value represents the average sum of several values which may not all be represented by a first order oxidation reaction (eq 1). On the basis of a comparison to the E_a reported for oxidation of poly(methylsilsesquioxane) (20.5 kcal/mol),[32] we believe that the average value of E_a obtained from the direct method (20 ± 4 kcal/mol) is more realistic than that computed with the indirect method.

The paucity of E_a data for silsesquioxanes is surprising given their great utility.[33] The activation energies for poly(phenylsilsesquioxane) and poly(methylsilsesquioxane) under nitrogen have only recently been reported and were determined to be 64.5[21] and 28.5 kcal/mol.[32] The value for the poly(phenylsilsesquioxane) is in agreement with that listed for the POSS−siloxane copolymer in Table 2. In addition, the data in Table 2 clearly reveal that activation energies in aggressive atmospheres are approximately 3-fold lower than those in an inert atmosphere.

Surface Area, Porosity, and Density Determinations. During the pyrolysis of a char-forming polymer, the material undergoes a number of physical transformations aside from those of a primarily chemical nature mentioned above. To provide insight into these aspects of the thermolysis process, a series of surface area and density measurements were made at intermediate stages during the pyrolysis of the [$Cy_8Si_8O_{11}$−$(OSiMe_2)_{5.4}O$−] copolymer.

The dependence of surface area and density on pyrolysis temperature are shown in Figures 14 and 15. The surface areas were computed from the nitrogen

(30) This assumes the decomposition reaction is a first-order reaction.

(31) Ismail, I. M. K.; Rodgers, S. L. *Carbon* **1992**, *30*, 229.

(32) Li, D.; Hwang, S.-T. *J. Appl. Polym. Sci.* **1992**, *44*, 1979.

(33) For example see: Baney, R. H.; Itoh, M.; Sakakibara, A.; Suzuki, T. *Chem. Rev.* **1995**, *95*, 1409.

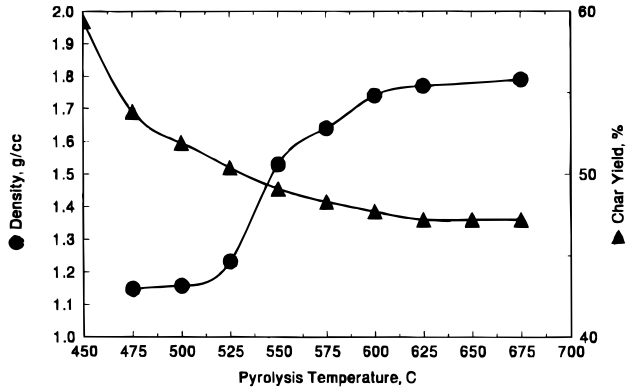

Figure 14. Plot of density and mass loss vs temperature for $[Cy_8Si_8O_{11}-(OSiMe_2)_{5.4}O-]$.

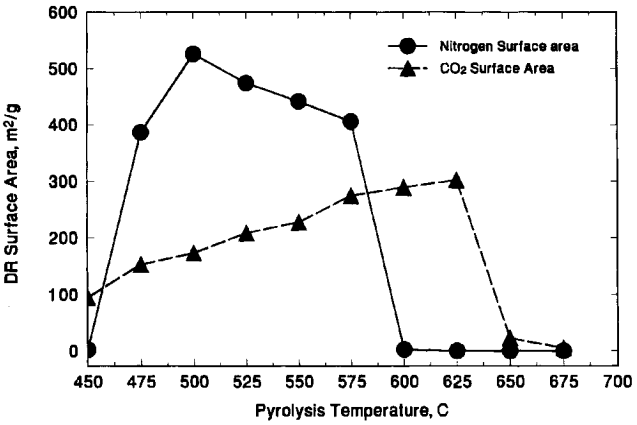

Figure 15. Plot of surface area vs pyrolysis temperature for $[Cy_8Si_8O_{11}-(OSiMe_2)_{5.4}O-]$.

isotherm using the Brunauer–Emmett–Teller (BET) equation[11] and from CO_2 isotherms using the Dubinin–Radushkivich (DR) equation.[13] With CO_2 adsorption at 30 °C, the adsorbate molecules can access micropores that, with some char samples, could not be accessed by nitrogen at −196 °C. Due to the differences in adsorption temperature, the diffusion of CO_2 inside the micropores at 30 °C is considerably faster than N_2 at −196 °C. In this case, only the micropore surface area and micropore volume are estimated with this gas using the DR equation. Therefore, the nitrogen surface areas obtained here for each of the partially pyrolyzed polymer samples can be approximated as the sum of meso- and micropore areas. Note that some macropores were also observed using SEM. Both surface and density measurements were taken on samples that were exposed to a (stepwise) isothermal pyrolysis rather than through the temperature ramped TGA experiments (Figures 4 and 5).

Figure 14 shows that heating the polymer to 450 °C results in the loss of approximately 40% of the starting polymer weight. At this point in pyrolysis, the density of the char residue (Figure 14) is 1.1 g/cm^3 and is surprisingly comparable to that of the starting polymer; 1.12 g/cm^3. Only minimal porosity can be observed in the char at this temperature (Figure 15). At 475 °C, a major change in porosity and an abrupt increase in micro- and mesopore surface areas were noted. At 500 °C, an additional 10% weight loss was observed and the density of the char began increasing as the total porosity (micro-plus mesoporosity) was maximized. At this stage in the pyrolysis, the sample was no longer white and appeared as a black solid. Continued heating from 500 to 675 °C resulted in a char density increase to 1.79 g/cm^3. Over this region, an additional ∼4% of the starting polymer weight was lost. Further heating to 1000 °C maximized the char density to 1.96 g/cm^3.

The porosity, surface area, and density measurements show that char densification takes place after the majority of mass loss from pyrolysis has occurred. Once the maximum density has been reached, pore closure occurs between 600 and 650 °C and the surface area decreases from 406 to 2.5 m^2/g. Continued heating from 650 to 1000 °C had little effect on density and porosity of the char. Microporosity in Si–O–C chars heated to 1000 °C has similarly been achieved from the pyrolysis of networks prepared from octafunctional spherosilicate precursors.[34] The ability of POSS-based polymers to form microporous chars may lend them useful as precursors to membranes and in thermal protection applications.

Conclusions

Both fully and incompletely condensed POSS macromers sublime upon attempted thermolysis provided they contain functionalities which do not readily undergo cross-linking reactions. Retention of the initial POSS structure in the sublimates is observed even for incompletely condensed structures. Once incorporated into a polymeric form, POSS macromers do not sublime; rather they decompose primarily through partial loss of their organic substituents followed by subsequent cross-linking reactions which incorporates the remaining composition into an SiO_xC_y network (char). Similar decomposition processes involving partial loss of organic substituents followed by the formation of SiOC networks have been observed in related polysilsesquioxane resins.[4] Such a pathway would in fact seem to be preferred when the relative silicon–oxygen and silicon–carbon bond strengths are considered and provided that some cross-linking can occur to prevent a significant loss of silicon–oxygen containing fragments.

Thermolysis of the POSS monomers and polymers does result in changes to the silicon–oxygen "cage" structure. For monomers such as $Cy_8Si_8O_{11}(OH)_2$ which contain silanol groups, decomposition initially occurs through loss of T-type silanol silicon environment presumably through elimination of H_2O. Monomer decomposition then proceeds via an intermediate composed primarily of T-type silicon environments. Further decomposition occurs through loss of the organic substituents and heating past 450 °C results in scrambling of the silicon environment and the formation of SiO_xC_y-based chars containing variable amounts of D, T, and Q structure. Decomposition of POSS–siloxane copolymers initially occurs through depolymerization of the oligomeric poly(dimethylsiloxane) comonomer segment, followed by the loss of hydrocarbons. This is in stark contrast to the reported evolution of fully condensed $[MeSiO_{1.5}]_n$ from methylsilicone resins. As was observed for the POSS macromer, retention of the initial POSS silicon–oxygen framework is retained only during the initial stages of pyrolysis (approximately up to 500 °C).

(34) Agaskar, P. A. *J. Chem. Soc., Chem. Commun* **1992**, 1024.

Further heating results in scrambling of the silicon environment.

Chars resulting from the pyrolysis of the POSS−siloxane polymers begin to develop their structural foundation as the evolution of the gaseous pyrolysis products nears completion. The density and porosity of the char foundation becomes stable near 650 °C. Activation energies for pyrolysis (56 kcal/mol) and oxidation (20 kcal/mol) of the POSS-based compositions are comparable to what has been previously observed for polysilsesquioxanes.

Acknowledgment. We thank the Air Force Office of Scientific Research, Chemistry and Life Sciences Directorate, and the Phillips Laboratory Propulsion Directorate for financial support. Appreciation is also expressed to Ms. Yoshiko Otonari for assistance with the NMR experiments and synthesis of $Cy_8Si_8O_{12}$. Appreciation is also given to Dr. Tom Wittberg of the University of Dayton Research Institute for the XPS analysis of char samples.

CM950536X